# DPSK PERFORMANCE OF A CODED SSMA SYSTEM WITH MICRODIVERSITY IN A NAKAGAMI FADING ENVIRONMENT

Pieter van Rooyen

Department of Electrical and Electronical Engineering, University of Pretoria, Pretoria, 0002, South Africa

## Abstract

This work considers the performance of Direct Sequence Spread Spectrum Multiple Access (DS/SSMA) transmission with MRC diversity for cellular indoor wireless communication (IWC) channels, although it is not entirely restricted to the IWC channel. The indoor communication channel, which is multipath faded, is modelled by a discrete set of Nakagami faded paths. The Nakagami fading distribution has been shown to fit empirical results more generally than other distributions [1]. New analytical results to evaluate the probability of error for the receiver terminals studied in this work are presented. Numerical results reveal that for nondiversity receivers, Nakagami fading is very hostile to the SSMA signal. However, with the use of MRC diversity, interleaving and convolutional coding, the average error rate can be reduced dramatically, allowing for reliable communication.

## 1 Introduction

Spread spectrum signalling techniques, with its inherent anti- multipath, multiple access and rejection of interference capabilities have increasingly received attention for cellular personal and mobile communications. Until recently the standard analysis of SSMA systems was rather pessimistic about the capacity of these systems compared to FDMA and TDMA. Gilhousen et al [2] recognized that since SSMA capacity is only interference limited (unlike FDMA and TDMA) any reduction in interference converts directly and linearly into an increase in capacity. Therefore, by employing a voice activity factor, sectorizing the cells and using various forms of diversity it is possible to achieve SSMA system capacity at least as good as FDMA and TDMA. This improvement has been indicated by [2] and others under AWGN conditions.

In this paper a detailed analysis of the performance of a cellular SSMA system with diversity under frequency-selective slowly fading Nakagami and multipath conditions is presented. For diversity purposes MRC and convolutional coding are considered. Coherent PSK is assumed as modulation scheme and consequently the analysis can be applied to the downlink of a cellular SSMA system.

There is a sizable literature relating to the effects of multiple access interference on the performance of cellular DS-SSMA, among which are [3] and [4]. Most literature, except Xiang [3], assume either Rayleigh or Rician fading statistics to model the IWC channel. It has been shown, however, that the Nakagami-$m$ distribution assumes the signals are received with random moduli and phases, leading to more flexibility in matching experimental data than that of Rayleigh or Rice models, i.e. [5] and [6] to mention a few. This is especially true for the indoor wireless and densely built urban channels.

Using the equations derived in this work it is possible to predict DS/SSMA capacity under the mentioned conditions with MRC and convolutional coding. By introducing a voice activity factor of 3/8 and cell splitting of 3, the performance of a cellular system is assessed. It is assumed that hard decisions are made by the demodulator and that the error- producing mechanism results in independent error events. The latter assumption requires interleaving at the transmitter and de-interleaving at the receiver.

Section 2 analyses and describes a system model for a typical indoor wireless communication channel. The analyses allows for the calculation of the average error probabilities by means of closed form expressions, making use of the Gaussian Assumption to model the multiple access interference. The bounds used to calculate the convolutional coded performance is presented in Section 3. Numerical results are discussed in Section 4 and finally, conclusions are presented in the last section of the paper.

## 2 System model and evaluation

The model considered will be summarized briefly and is based on the model developed by Kavehrad [4].

Measurements by Qualcomm [7] indicate that the adjacent cell interference in a cellular system contribute approximately 50% of the total interference (for equally loaded cells). Therefore, assuming equally loaded cells, the maximum number of users a cellular system can support is given by

$$K' = K\frac{N_{sect}}{V_{on}}1.5 \qquad (1)$$

where $K$ is the total number of users per cell, $V_{on}$ the voice activity factor and $N_{sect}$ the cell splitting factor. Our conjectural system will assume $\frac{N_{sect}}{V_{on}} = 8$.



0-8186-7075-4/95 $04.00 © 1995 IEEE

The channel for the desired transmitter and receiver ($k = 1$) can be represented by an $L$-paths Nakagami fading model where a single transmitted pulse is received via $L$-paths at the random instant $t_l, l = 1, \cdots, L$. We assume $t_l$ is uniformly distributed over one bit period $(0, T)$ and that each user code sequence has a period of $N = T/T_c$.

In the analysis we assume that average power control is assumed which also includes averaging the channel fading characteristics. Baseband signalling at a rate less than the channel coherence bandwidth ensures that intersymbol interference can be neglected. Therefore, the channel has a low-pass equivalent impulse response, given by

$$h(t) = \sum_{l=1}^{L} \beta_l \delta(t - t_l) e^{j\phi_l}, \tag{2}$$

where $\delta(\cdot)$ is the delta function, $\beta_l$ is the Nakagami distributed path gain and $\phi_l$ is the random path phase, uniformly distributed between $(0, 2\pi]$.

In the transmission model it is further assumed that the $k$th interfering user of the multiple access system is linked to the receiver via a single Nakagami fading path with a uniformly distributed random delay $\tau_k$ ranging from zero to one bit period, $T$. This will naturally result in a worst case scenario, rendering the results conservative.

In our formulation we specify the Nakagami distributed path gain of the $K - 1$ interfering users by $V_k, k = 2, \cdots, K$. Thus, the received signal for the fading model described is given by

$$\begin{aligned} r(t) &= A \sum_{l=1}^{L} \beta_l a_1(t - t_l) b_1(t - t_l) \cos(\omega_c t + \Phi_l) \quad (3) \\ &+ A \sum_{k=2}^{K} V_k a_k(t - \tau_k) b_k(t - \tau_k) \cos(\omega_c t + \Psi_k) \\ &+ n_c(t) \cos(\omega_c t) + n_s(t) \sin(\omega_c t) \end{aligned}$$

where $\Phi_l = \theta_1 - \omega_c t_l + \phi_l$, $\Psi_k = \theta_k - \omega_c \tau_k$ and $\theta_k$ the phase of the $k$th user. Also, $n(t)$ has been expressed in terms of its lowpass equivalent components $n_s(t)$ and $n_c(t)$ [8]. The carrier phase $\theta_k$ has been absorbed in the random phase $\phi_k$ associated with each channel path.

We arbitrarily choose user $k = 1$ as the reference user and calculate the probability of error of the data symbol $b_0^1$. At time $t = T$, the nominal sampling point for matched filter detection, we have [9]

$$\begin{aligned} \zeta_c(T) &= A \sum_{l=1}^{L} \beta_l \left\{ b_{-1}^1 R_{1,1}(t_l) + b_0^1 \hat{R}_{1,1}(t_l) \right\} \cos\phi_l \quad (4) \\ &+ A \sum_{k=2}^{K} V_k \left\{ b_{-1}^k R_{k,1}(\tau_k) + b_0^k \hat{R}_{k,1}(\tau_k) \right\} \cos\phi_k \\ &+ \eta, \end{aligned}$$

and

$$\begin{aligned} \zeta_s(T) &= A \sum_{l=1}^{L} \beta_l \left\{ b_{-1}^1 R_{1,1}(t_l) + b_0^1 \hat{R}_{1,1}(t_l) \right\} \sin\phi_l \quad (5) \\ &+ A \sum_{k=2}^{K} V_k \left\{ b_{-1}^k R_{k,1}(\tau_k) + b_0^k \hat{R}_{k,1}(\tau_k) \right\} \sin\phi_k \\ &+ \nu, \end{aligned}$$

with the definitions of $b_0^k$, $b_{-1}^k$, $R_k(\tau)$ and $\hat{R}_k(\tau)$ as defined in [10], and

$$\eta = \int_0^T a_1(s) n_c(s) ds, \tag{6}$$

and

$$\nu = \int_0^T a_1(s) n_s(s) ds. \tag{7}$$

The noise samples $\eta$ and $\nu$ are independent zero-mean Gaussian random variables with equal variance $\sigma_n^2 = N_0 T$ [11]. Notice that, as in the coherent case, the intersymbol interference here is due to partial correlation and involves only the previous bit. For most indoor channels, the delay spread is considerably less than the bit intervals of practical interest and the partial correlation intersymbol interference is the only type present.

Now, let us assume without loss of generality that $t_1 = 0$ and $\phi_1 = 0$. That is, we assume that the first path ($L = 1$) between the transmitter of user 1 and the corresponding receiver is the reference path and all other paths constitute interference. Let $z_1$ denote the complex envelope of the matched filter output at the sampling instant, i.e. $z_1 = \zeta_c(T) + j\zeta_s(T)$. Since the fading is slow compared to the data rate, we may assume that the corresponding complex envelope at the previous sampling instant, denoted $z_2$, differs from $z_1$ only in the data bits involved and in the additive Gaussian noise samples. It is therefore easily shown that

$$\begin{aligned} z_1 &= \beta_1 A T b_0^1 \quad (8) \\ &+ AT \left\{ \sum_{l=2}^{L} \beta_l X_l \cos\phi_l + \sum_{k=2}^{K} V_k X_k \cos\phi_k \right\} \\ &+ jAT \left\{ \sum_{l=2}^{L} \beta_l X_l \sin\phi_l + \sum_{k=2}^{K} V_k X_k \sin\phi_k \right\} \\ &+ (\eta_1 + j\nu_1), \end{aligned}$$

and

$$z_2 = \beta_1 A T b_{-1}^1 \tag{9}$$

$$
\begin{aligned}
&+ \quad AT\left\{\sum_{l=2}^{L}\beta_l Y_l \cos\phi_l + \sum_{k=2}^{K} V_k Y_k \cos\phi_k\right\} \\
&+ \quad jAT\left\{\sum_{l=2}^{L}\beta_l Y_l \sin\phi_l + \sum_{k=2}^{K} V_k Y_k \sin\phi_k\right\} \\
&+ \quad (\eta_2 + j\nu_2),
\end{aligned}
$$

with

$$
\begin{aligned}
X_l &= b^1_{-1} R_{1,1}(t_l) + b^1_0 \hat{R}_{1,1}(t_l) \qquad (10)\\
X_k &= b^k_{-1} R_{k,1}(\tau_k) + b^k_0 \hat{R}_{k,1}(\tau_k)\\
Y_l &= b^1_{-2} R_{1,1}(t_l) + b^1_{-1} \hat{R}_{1,1}(t_l)\\
Y_k &= b^k_{-2} R_{k,1}(\tau_k) + b^k_{-1} \hat{R}_{k,1}(\tau_k).
\end{aligned}
$$

In (9), the data bit $b^k_{-2}$ of the $k$th user is transmitted two-bit intervals prior to $b^k_0$. The noise variables $\eta_1$, $\eta_2$, $\nu_1$ and $\nu_2$ are independent of one another, and the binary data bits are equal to $+1$ or $-1$ with equal probability. The output of the DPSK demodulator at the sampling instant is given by

$$
\zeta = \mathrm{Re}[z_1 z_2^*], \qquad (11)
$$

where * denotes complex conjugate.

Let us indicate the transmitted DPSK signals as $s_1(t)$ and $s_2(t)$. In relation to the received signal, $z_1(t)$ and $z_2(t)$, the following binary signal pair is transmitted

$$
\begin{aligned}
s_1(t) &= (z_1(t), z_1(t)) \quad \text{or} \quad (z_2(t), z_2(t)) \qquad (12)\\
s_2(t) &= (z_1(t), z_2(t)) \quad \text{or} \quad (z_2(t), z_1(t))
\end{aligned}
$$

As explained before, the first $T$ seconds of each waveform are actually the last $T$ seconds of the previous waveform. Note that $s_1(t)$ and $s_2(t)$ can each have either of two possible forms and that $z_1(t)$ and $z_2(t)$ are antipodal signals. Therefore, pairs of DPSK signals can be represented as orthogonal signals $2T$ long. Detection could correspond to noncoherent envelope detection with four channels matched to each of the possible envelope outputs. Since the two envelope detectors representing each symbol are negatives of each other, the envelope of each will be the same. Hence the detectors can be implemented as a single channel matched to $s_1(t)$ or $s_2(t)$.

The probability of error can now be calculated by realizing that

$$
P_e = P(\zeta > s_2 | z_2). \qquad (13)
$$

For the case where $z_2(t)$ is sent, the output of $z_1(t)$ will be only Gaussian noise, and therefore the output of the envelope detector is noise having a Rayleigh distribution, given by

$$
p_{z_1|s_2} = \frac{z_1}{\sigma_n^2}\exp\left\{-\frac{z_1^2}{2\sigma_n^2}\right\} \qquad \forall \qquad z_1 \geq 0, \quad (14)
$$

where $\sigma_n^2$ is the noise at the filter output.

On the other hand $z_2(t)$ has a Rice distribution since the input to the envelope detector is Gaussian noise plus a signal component. The pdf is written as

$$
p(z_2|s_2) = \frac{z_2}{\sigma_n^2}\exp\left\{-\frac{z_2^2 + m_2^2}{2\sigma_n^2}\right\} I_o\left(\frac{z_2 m_2}{\sigma_n^2}\right) \qquad (15)
$$

with

$$
m_2 = \frac{(\beta_1 + \alpha)AT}{2}, \qquad (16)
$$

which is the average of the Gaussian decision variable.

Now, when $s_2$ is transmitted, the receiver makes an error whenever the envelope sample $z_1(t)$ exceeds the envelope sample $z_2(t)$. Thus the probability of this error can be obtained by integrating $p(z_1|s_2)$ with respect to $z_1(t)$ from $z_2(t)$ to infinity, and then averaging over all possible values of $z_2(t)$. That is,

$$
\begin{aligned}
P_e &= \int_0^\infty p(z_2|s_2)\left\{\int_{z_2}^\infty p(z_1|s_2)dz_1\right\} dz_2 \qquad (17)\\
&\int_0^\infty \frac{z_2}{\sigma_n^2}\exp\left\{-\frac{z_2^2+m_2^2}{2\sigma_n^2}\right\} I_o\left(\frac{z_2 m_2}{\sigma_n^2}\right)\\
&\qquad \left\{\int_{z_2}^\infty \frac{z_1}{\sigma_n^2}\exp\left\{-\frac{z_1^2}{2\sigma_n^2}\right\} dz_1\right\} dz_2.
\end{aligned}
$$

Using integration tables by [12], the integral in (17) is evaluated analytically as

$$
P_e = \frac{1}{2}\exp\left\{-\frac{m_2^2}{2\sigma^2}\right\} \qquad (18)
$$

After substituting (16) in (17) we have an expression for the conditional error rate for DPSK signalling

$$
P_{e|\beta_1,\alpha} = \frac{1}{2}\exp\left\{-(\beta_1+\alpha)^2\frac{E_b}{N_0}\right\}. \qquad (19)
$$

The conditioning in $\alpha$ can be removed by the integration

$$
P_{e|\beta_1} = \int_{-\infty}^{\infty} P_{e|\beta_1,\alpha}\, p(\alpha) d\alpha \qquad (20)
$$

where $p(\alpha)$ is a zero mean Gaussian distribution. The result after integration is

$$P_{e|\beta_1} = \frac{1}{2}\exp\left(-\Lambda\beta_1^2\frac{E_b}{N_0}\right) \tag{21}$$

with

$$\frac{1}{\Lambda} = 1 + 2\frac{E_b}{N_0}\sigma_{ma}^2 \tag{22}$$

and $\sigma_{ma}^2$, the variance of $\alpha$, obtained from the correlation parameters of the spreading sequences.

Using

$$\overline{\gamma}_b = E\{\beta_i^2\}\frac{E_b}{N_0}, \tag{23}$$

$$p(\gamma_b) = \left(\frac{m}{\overline{\gamma}_b}\right)^{\epsilon}\frac{\gamma_b^{\epsilon-1}}{\Gamma(\epsilon)}\exp\left(-\frac{m\gamma_b}{\overline{\gamma}_b}\right) \quad \forall \quad \gamma_b \geq 0, \tag{24}$$

and $\epsilon = mP$ ($m$ the Nakagami fading parameter and $P$ the number of diversity branches) the conditioning in $\beta_1$ of (21) can be removed.

The result after integration by parts is

$$P_e = \frac{1}{2}\left(1 + \frac{\gamma_0\Lambda}{m}\right)^{-\epsilon}, \tag{25}$$

which is the result for DPSK SSMA signalling under Nakagami fading.

Without multiple access interference and $m = 1$, (25) reduces to

$$P_e = \frac{1}{2}\left\{\frac{1}{1+\gamma_0}\right\} \tag{26}$$

which is the well known performance of a single-path Rayleigh fading channel, i.e. [13].

As $m \to \infty$ and $P = 1$, that is no fading, and using the identity [12]

$$\lim_{m\to\infty}\left(1 + \frac{z}{m}\right)^{-m} = \exp(-z) \tag{27}$$

it is easily shown that

$$\lim_{m\to\infty}\frac{1}{2}\left(1 + \frac{\gamma_0\Lambda}{m}\right)^{-\epsilon} = \frac{1}{2}\exp\left\{\left(\frac{N_0}{E_b} + 2\sigma_{ma}^2\right)^{-\frac{1}{2}}\right\}, \tag{28}$$

which is similar to an expression derived at under non-fading conditions [14].

## 3 Channel Coding

Error control coding can be used with great success in SSMA with no penalty paid in bandwidth by the addition of redundancy to the information bits. It is further shown that low rate coding can be used very efficiently in a SSMA system. In this work rate $R_{cd} = \{\frac{1}{2}, \frac{1}{4}, \frac{1}{8}\}$ constrained length $\nu = \{2,3,4\}$ convolutional codes are considered.

It is assumed that the PN spreading sequence spans one code symbol. This implies that under the assumption of fixed throughput (i.e. constant data rate), fixed maximum chip rate and fixed complexity, a rate $R_{cd}$ code must employ a PN spreading sequence shorter by a factor $R_{cd}$ than that of the uncoded case. This results in increased interuser interference due to the poorer cross correlation properties of shorter PN sequences. In our case we use PN sequences of $N = 511$ for the uncoded case and $N = 255, 127$ and 63 for rate $R_{cd} = \{\frac{1}{2}, \frac{1}{4}, \frac{1}{8}\}$ codes respectively.

The Chernoff bound, as indicated in [13], is used to derive performance results, and is given by

$$P_b \leq \sum_{d=d_{free}}^{\infty} a_d P_2(d), \tag{29}$$

with $P_2(d)$ is the pairwise error probability as indicated in [13] and the coefficients $\{a_d\}$ related to the number of paths corresponding to the set of distances $\{d\}$.

## 4 Numerical Results

In the subsequent evaluations, with no loss of generality, the normalization $\Omega = -10$ dB is adopted so that the received energy in the fading channel, $\beta_1^2 E_b$, has an average value $E\{\beta_1^2 E_b\} = \Omega E_b = 0.1E_b$. With $\Omega = 0.1$, the Nakagami pdf is reduced to a one-parameter distribution so that all the results can be expressed in terms of the single parameter $m$. To investigate the influence of the Nakagami parameter $m$, five values are investigated; $m = \{\frac{1}{2}, 1, 2, 3, 5\}$. For $m = 1$ the Nakagami pdf reduces to the Rayleigh pdf and hence can be used for benchmark purposes. The parameter $m$ is inversely proportional to the amount of fading. In other words, as $m$ increases the pdf tends to an impulse response and consequently represents no fading.

### 4.1 Nakagami Performance without Diversity

Figure 1 indicates the performance for $K = 2$ and $L = 1$. It is apparent that the average error rate decreases substantially as $m$ increases. For $m = \frac{1}{2}$, severest fading, the performance for as little as two users is very poor and saturates at an error rate of $10^{-2}$ and consequently the system fails as a multiple access system for $m < 1$.

Table 1 indicates the capacity of a Nakagami faded SSMA system for different values of $m$ and $L$ at $E_b/N_0 = 50$ dB. The case $m = \infty$ represents the unfaded performance and also the value that the capacity of a Nakagami faded channel will saturate at.

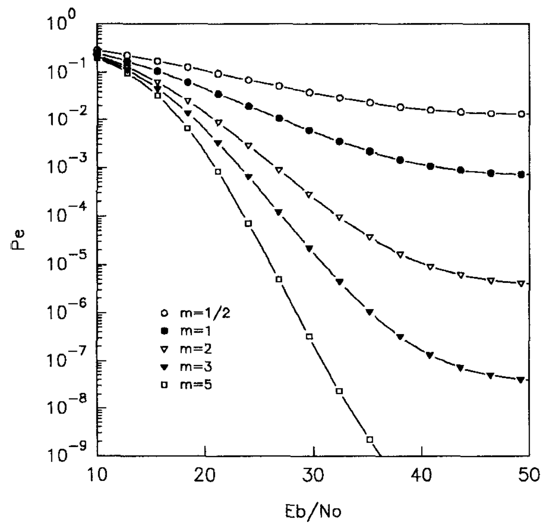


Figure 1: Nakagami faded DPSK performance: $K = 2$, $L = 1$ and $N = 511$

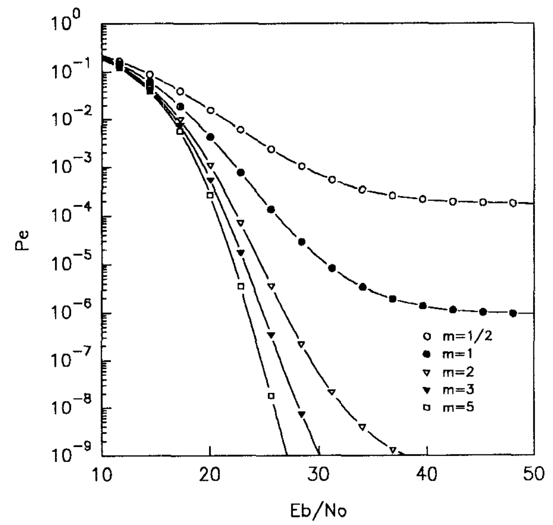


Figure 2: Nakagami faded DPSK performance: $K = 30$, $L = 3$, $P = 3$, $N = 511$ and $m = \{\frac{1}{2}, 1, 2, 3, 5\}$

Using Table 1 and (25) it is possible to calculate the capacity of a cellular system with voice activity monitoring and cell splitting. It is clear that by virtue of a cellular architecture it is possible to increase the system capacity by a factor of eight. However, the capacity of such a system is still relatively low and it is clear that some form of diversity is needed to substantially increase the system capacity, especially under multipath fading conditions.

## 4.2 Nakagami Performance with MRC Diversity

Figure 2 indicates the performance improvement by using a MRC receiver for $L = 3$ and a three branch

| | $P_e$ | $L=1$ | $L=5$ | $L=10$ |
|---|---|---|---|---|
| $m=1/2$ | $10^{-3}$ | - | - | - |
| $m=1$ | $10^{-3}$ | 2 | - | - |
| $m=2$ | $10^{-3}$ | 18 | 13 | 7 |
| | $10^{-5}$ | 2 | - | - |
| $m=3$ | $10^{-3}$ | 37 | 32 | 26 |
| | $10^{-5}$ | 8 | 2 | - |
| $m=5$ | $10^{-3}$ | 62 | 57 | 50 |
| | $10^{-5}$ | 20 | 15 | 8 |
| | $10^{-8}$ | 5 | - | - |
| $m=\infty$ | $10^{-3}$ | 115 | - | - |
| | $10^{-5}$ | 63 | - | - |
| | $10^{-8}$ | 36 | - | - |

Table 1: $K$ for non-diversity DPSK: $E_b/N_0 = 60$ dB, $P = 1$ and $L = \{1, 5, 10\}$

($P = 3$) diversity receiver for $K = 30$. For $m = \frac{1}{2}$ and a three tap MRC receiver the average error rate is decreased substantially, ensuring at least $K = 30$ at an error rate of $10^{-3}$.

As benchmark, the performance for $m = 1$ is also indicated in Figure 2. Again the performance is substantially improved as the number of taps, $P$, increases. For a three tap MRC receiver with $m = 1$, the performance is approximately three orders better than for the $m = \frac{1}{2}$ case.

Figure 3 indicates the capacity, $K$, as a function of $P$ for different values of $m$. We therefore note that the capacity saturates to less than a 1000 users as $P$ increases.

Table 2 indicates the capacity of a single cell Nakagami faded system with MRC diversity up to five branches. A linear increase in $K$ with $P$ is noticeable. As before, the cellular capacity can be obtained by multiplying the indicated values by a factor of five when voice activity and sectorization are included.

## 4.3 Nakagami Performance with Convolutional Coding

As another form of diversity, we consider the performance of a SSMA system under Nakagami fading with convolutional coding. As mentioned before, coding can be implemented very efficiently in a spread spectrum system. Table 3 indicates the capacity improvement due to rate $R_{cd} = \{\frac{1}{2}, \frac{1}{4}, \frac{1}{8}\}$ convolutional codes with constrained length $\nu = 4$.

It is interesting to note that low rate coding becomes effective as $m$ increases. In other words if the channel is highly faded, i.e. $m = \frac{1}{2}$, low rate convolutional coding can be used to increase system capacity.

| | $P_e$ | $P=2$ | $P=3$ | $P=4$ | $P=5$ |
|---|---|---|---|---|---|
| | $10^{-3}$ | 2 | 3 | 68 | 134 |
| $m=1/2$ | $10^{-5}$ | - | - | 3 | 16 |
| | $10^{-3}$ | 35 | 108 | 202 | 305 |
| $m=1$ | $10^{-5}$ | 3 | 19 | 51 | 94 |
| | $10^{-8}$ | - | - | 6 | 18 |
| | $10^{-3}$ | 102 | 208 | 322 | 439 |
| $m=2$ | $10^{-5}$ | 27 | 73 | 130 | 191 |
| | $10^{-8}$ | 4 | 19 | 43 | 73 |
| | $10^{-3}$ | 139 | 254 | 372 | 492 |
| $m=3$ | $10^{-5}$ | 49 | 75 | 171 | 236 |
| | $10^{-8}$ | 13 | 39 | 72 | 108 |
| | $10^{-3}$ | 177 | 296 | 416 | 537 |
| $m=5$ | $10^{-5}$ | 78 | 142 | 210 | 277 |
| | $10^{-8}$ | 30 | 65 | 104 | 143 |

Table 2: $K$ for MRC diversity DPSK: $E_b/N_0 = 60$ dB, $P = \{2,3,4,5\}$ and $L = \{2,3,4,5\}$

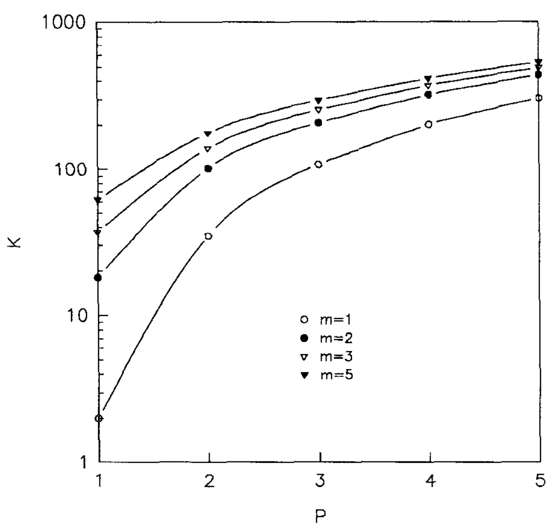


Figure 3: Capacity of a $P$ branch system

| | $P_e$ | $\nu=2$ | $\nu=3$ | $\nu=4$ |
|---|---|---|---|---|
| | $10^{-3}$ | 4 | 11 | 35 |
| $m=1/2$ | $10^{-5}$ | - | 2 | 16 |
| | $10^{-8}$ | - | - | 6 |
| | $10^{-3}$ | 28 | 28 | 61 |
| $m=1$ | $10^{-5}$ | 9 | 14 | 36 |
| | $10^{-8}$ | 2 | 6 | 19 |
| | $10^{-3}$ | 68 | 44 | 78 |
| $m=2$ | $10^{-5}$ | 35 | 27 | 52 |
| | $10^{-8}$ | 14 | 15 | 33 |
| | $10^{-3}$ | 89 | 58 | 85 |
| $m=3$ | $10^{-5}$ | 52 | 33 | 58 |
| | $10^{-8}$ | 26 | 20 | 38 |
| | $10^{-3}$ | 110 | 56 | 90 |
| $m=5$ | $10^{-5}$ | 71 | 38 | 63 |
| | $10^{-8}$ | 40 | 25 | 43 |
| | $10^{-3}$ | 135 | 122 | 98 |
| $m=\infty$ | $10^{-5}$ | 94 | 85 | 69 |
| | $10^{-8}$ | 62 | 57 | 48 |

Table 3: $K$ for convolutional coded DPSK at $E_b/N_0 =$ 60 dB, $P=1$, $L=1$, $R_{cd} = \frac{1}{8}$ and $N = 63$

However, as $m = \infty$, that is no fading, half rate coding is the most effective.

### 4.4 Nakagami Performance with MRC Diversity and Coding

It is shown that low rate convolutional coding is not very effective when $m$ is small. Therefore, Table 4 indicates only the performance of half rate convolutional codes combined with a $P$ branch diversity receiver. The performance is greatly enhanced by a combination of coding and diversity. The improvement over the uncoded, non-diversity case is 909% at $m = 5$, $P = 5$ and $P_e = 10^{-3}$.

From this table it is clear that a combination of convolutional coding and MRC diversity is very effective in enhancing the capacity. Moreover, combining error control codes and diversity is bandwidth and power efficient since the average error rate saturates at lower values of $E_b/N_0$.

## 5 Conclusions

From the preceding results it is apparent that Nakagami fading with small values of $m$ is very hostile to a SSMA signal. Using diversity, specifically RAKE reception and convolutional coding, it is possible to increase the capacity of a Nakagami faded SSMA signal substantially.

| | $P_e$ | $P=2$ | $P=3$ | $P=4$ | $P=5$ |
|---|---|---|---|---|---|
| $m=1/2$ | $10^{-3}$ | 54 | 150 | 267 | 395 |
| | $10^{-5}$ | 17 | 66 | 136 | 217 |
| | $10^{-8}$ | 2 | 18 | 51 | 94 |
| $m=1$ | $10^{-3}$ | 135 | 265 | 401 | 541 |
| | $10^{-5}$ | 69 | 153 | 247 | 344 |
| | $10^{-8}$ | 26 | 74 | 131 | 194 |
| $m=2$ | $10^{-3}$ | 202 | 342 | 484 | 628 |
| | $10^{-5}$ | 124 | 223 | 323 | 425 |
| | $10^{-8}$ | 67 | 131 | 198 | 267 |
| $m=3$ | $10^{-3}$ | 229 | 371 | 515 | 658 |
| | $10^{-5}$ | 149 | 250 | 352 | 455 |
| | $10^{-8}$ | 88 | 156 | 225 | 296 |
| $m=5$ | $10^{-3}$ | 252 | 396 | 540 | 684 |
| | $10^{-5}$ | 171 | 274 | 377 | 480 |
| | $10^{-8}$ | 108 | 178 | 249 | 320 |

Table 4: $K$ for convolutional coded and MRC diversity DPSK, $R_{cd} = \frac{1}{2}$, $\nu = 4$ and $N = 255$

Convolutional coding is probably a simpler means to obtain diversity, but has the drawback that interleaving is required. Especially in a speech based system interleaving can lead to excessive and unacceptable delays. RAKE reception on the other hand is more complex, but with advances in ASIC technology, this problem can be surmounted in the near future.

To conclude, to guarantee acceptable performance under Nakagami fading conditions some form or forms of diversity is absolutely necessary - the type of diversity needed is to be dictated by the specific application and cost considerations.

## References


[1] U. Charash, "Reception through Nakagami fading multipath channels with random delays," *IEEE Transactions on Communications*, vol. COM-27, pp. 657–670, April 1979.

[2] K. Gilhousen, I. Jacobs, R. Padovani, and L. Weaver, "Increased capacity using CDMA for mobile satellite communications," *IEEE Transactions on Selected Areas in Communication*, vol. 8, pp. 503–514, May 1990.

[3] H. Xiang, "Binary Code-Division Multiple-Access Systems operating in Multiple Fading, Noisy channels," *IEEE Transactions on Communications*, vol. COM-33, no. 8, pp. 775–784, August 1985.

[4] M. Kavehrad, "Performance of Nondiversity Receivers for spread spectrum in Indoor Wireless Communications," *AT&T Technical Journal*, vol. 64, no. 6, pp. 1181–1210, July-August 1985.

[5] M. A. Mokhtar and C. Gupta, "Power control considerations for DS/CDMA personal communication systems," *IEEE Transactions on Vehicular Technology*, vol. 41, pp. 479–487, November 1992.

[6] P. Crepeau, "Uncoded and coded performance of MFSK and DPSK in Nakagami fading channels," *IEEE Transactions on Communications*, vol. 40, pp. 487–493, March 1992.

[7] "An overview of the application of CDMA to digital cellular systems and personal cellular networks," tech. rep., Qualcomm Inc., San Diego, Ca, May 1992.

[8] L. Couch, *Digital and analog communication systems.* Macmillan Publishing Co., 1983.

[9] M. Kavehrad and B. Ramamurthi, "Direct sequence spread spectrum with DPSK modulation and diversity for indoor wireless communications," *IEEE Transactions on Communications*, vol. COM-35, pp. 224–236, February 1987.

[10] M. Pursley, "Performance Evaluation for Phase-Coded SSMA Communications - Part 1: System Analysis," *IEEE Transactions on Communications*, vol. COM-25, no. 8, pp. 795–803, August 1977.

[11] B. Sklar, *Digital communications: Fundamentals and Applications.* Prentice Hall, 1988.

[12] M. Abramowitz and I. Stegman, *Handbook of Mathematical functions.* Washington, D.C.: National Bureau of Standards, 1964.

[13] J. Proakis, *Digital Communications.* McGraw-Hill, New York, 1983.

[14] G. L. Turin, "The Effects of Multipath and Fading on the Performance of Direct-Sequence CDMA Systems," *IEEE Journal on Selected Areas in Communications*, vol. SAC-2, pp. 597–603, July 1984.